

Article

A Novel Adaptive Neural Network-Based Thermoelectric Parameter Prediction Method for Enhancing Solid Oxide Fuel Cell System Efficiency

Yaping Wu ¹, Xiaolong Wu ^{2,3,4,*}, Yuanwu Xu ⁵, Yongjun Cheng ⁶ and Xi Li ^{2,3}

- ¹ College of Liberal Arts, Jiangxi Science and Technology Normal University, Nanchang 330000, China
² Belt and Road Joint Laboratory on Measurement and Control Technology, Huazhong University of Science and Technology, Wuhan 430074, China
³ Shenzhen Research Institute, Huazhong University of Science and Technology, Shenzhen 518055, China
⁴ School of Information Engineering, Nanchang University, Nanchang 330031, China
⁵ School of Information Science and Engineering, Wuhan University of Science and Technology, Wuhan 430081, China
⁶ Wuhan Maritime Communication Research Institute, Wuhan 430205, China
* Correspondence: wxl6895209@gmail.com

Abstract: Efficiency prediction plays a crucial role in the ongoing development of electrochemical energy technology. Our industries heavily depend on a reliable energy supply for power and electricity, and solid oxide fuel cell (SOFC) systems stand out as renewable devices with immense potential. SOFCs, as one of the various types of fuel cells, are renowned for their capability of combined heat and power generation. They can achieve an efficiency of up to 90% in operation. Furthermore, due to the fact that water is the byproduct of their electricity generation process, they are extremely environmentally friendly, contributing significantly to humanity's sustainable development. With the advancement of renewable energy technologies and the increasing emphasis on sustainable development requirements, predicting and optimizing the efficiency of SOFC systems is gaining importance. This study leverages data collected from an SOFC system and applies an improved neural network structure, specifically the dendritic network (DN) architecture, to forecast thermoelectric efficiency. The key advantage of this method lies in the adaptive neural network algorithm based on the dendritic network structure without manually setting hidden nodes. Moreover, the predicted model of thermoelectric efficiency is validated using 682 and 1099 h of operational data from the SOFC system, and the results are compared against a conventional machine learning method. After comparison, it is found that when the novel method with adaptive characteristics proposed was used for SOFC system efficiency prediction, the MAE and RMSE values were both lower than 0.014; the result is significantly better than from other traditional methods. Additionally, this study demonstrated its effectiveness in predicting the thermoelectric efficiency of SOFC systems through secondary experiments. This study offers guidance on enhancing SOFC systems thermoelectric efficiency. Therefore, this study provides a foundation for the future industrialization of fuel cell systems.

Keywords: solid oxide fuel cell system; thermoelectric efficiency; system efficiency; neural network



Citation: Wu, Y.; Wu, X.; Xu, Y.; Cheng, Y.; Li, X. A Novel Adaptive Neural Network-Based Thermoelectric Parameter Prediction Method for Enhancing Solid Oxide Fuel Cell System Efficiency. *Sustainability* **2023**, *15*, 14402. <https://doi.org/10.3390/su151914402>

Academic Editors: Mohammad Ali Abdelkareem, Hussein M. Maghrabia and Enas Taha Sayed

Received: 17 July 2023

Revised: 15 September 2023

Accepted: 25 September 2023

Published: 30 September 2023



Copyright: © 2023 by the authors. Licensee MDPI, Basel, Switzerland. This article is an open access article distributed under the terms and conditions of the Creative Commons Attribution (CC BY) license (<https://creativecommons.org/licenses/by/4.0/>).

1. Introduction

Renewable energy systems have had vigorous development in China. Renewable energy systems include other kinds of fuel cells such as solid oxide fuel cells (SOFCs) and proton exchange membrane fuel cells (PEMFCs) [1]. SOFC systems have broad application prospects because of their high thermoelectric efficiency (which includes heat efficiency and electrical efficiency), no noise, no pollution, and sustainability in power generation in vehicles and boats [2,3]. In addition, the global climate change has spurred a demand for

alternative fossil fuels, aimed at overcoming the environmental impacts of greenhouse gas emissions and limited resources [4]. Approaches such as waste heat recovery and green power generation technologies are being adopted to reduce dependence on conventional fossil fuels. SOFCs, serving as energy conversion devices, exhibit tremendous potential, characterized by not only compact size but also environmental friendliness. Furthermore, SOFCs can directly convert chemical energy into electricity, with water as a byproduct [5,6]. When integrated with cogeneration subsystems, SOFCs can enhance energy conversion efficiency, thus making a significant contribution to sustainable human development. Hence, high-efficiency forecasting for the SOFC cogeneration system is of paramount importance in ensuring stable operation and promoting sustainable environmental development (emission peak and carbon neutrality).

At present, the research on SOFC systems mostly focuses on the field of materials. However, in order to popularize SOFC systems, power generation efficiency is unavoidable. Especially in complex environments, a higher system efficiency results in a lower power generation cost. Furthermore, with the installation of a carbon capture device after the SOFC system, carbon dioxide emissions decrease significantly, having a positive impact on the environment and social development [7]. Therefore, some researchers have focused on improving SOFC system generation efficiency, so as to decrease energy loss and carbon dioxide emissions of SOFC systems [8].

In the field of system efficiency optimization, the main reliance is on mechanistic equations to build SOFC system models. For instance, Huo proposed a dynamic temperature model to control the SOFC stack temperature, simplifying it into a multi-input, multi-output nonlinear dynamic model for control. The accuracy of the proposed model in reflecting temperature dynamic characteristics is verified through simulation. Based on this model, an input-output feedback linearization controller is proposed to achieve the control goal [9]. Wu used a mechanism model for SOFC/PEMFC hybrid systems to improve energy efficiency and dynamic response capabilities. The model constructed incorporates the dominant mechanism of SOFCs' slow transient response on short-term dynamic behavior, and the results show that the proposed model has sufficient accuracy [10]. Although this method is feasible, it requires a significant amount of time for mechanism modeling. It is necessary to explore a new method to optimize SOFC system efficiency. Some scholars have used neural networks to evaluate fuel cell system performances. For example, Huo proposed a convolutional neural network method based on fuel cell I-V polarization curve output prediction, which has good fitting characteristics [11]. Wilberforce adopted a feedforward back propagation neural network to predict fuel cell voltage and current for assessing PEMFC cell performance [12]. Chen proposed a grey-box neural network model to predict fuel cell performance degradation and designed an experiment to verify the approach's effectiveness [13]. Xie proposed a modeling method to predict the reliability of fuel cells based on long-term and short-term memory recurrent neural networks, and the experiment proved its effectiveness [14]. From the literature above, neural networks have a wide application prospect in fuel cell performance prediction.

An artificial neural network simulates some basic characteristics of the human brain. It employs numerous simple units to simulate the structure and thinking processes of the human brain. The appropriate neural network type should meet the requirements of SOFC performance characteristics and accurate system efficiency prediction. For example, to improve efficiency from the perspective of microscale transmission, Buchanec et al. used constrained artificial neural networks to predict and reconstruct SOFC models. The results indicate that the model can accurately simulate the thermodynamic losses of anode electrodes [15]. Subotić designed a prediction framework based on an artificial neural network that is used to predict the SOFC polarization curve and electrochemical impedance spectroscopy [16]. Ba proposed a Hopfield neural network for identifying the SOFC model, which significantly reduces the time required for model identification, and the model fitting effect is excellent [17]. Gnatowski proposed a specialized calculation scheme based on artificial neural networks to accurately predict the overvoltage of

SOFC anodes, thereby constructing a functional relationship between temperature and current containing charge transfer coefficients, proving the effectiveness of artificial neural networks in high-precision modeling of SOFC electrochemical reactions [18]. Yan built a prediction model for SOFC stack cathode overpotential and degradation rate through artificial neural network and multi-objective optimization theory. Compared to the grid search method, Yan's proposed approach is more robust and efficient in optimizing the SOFC electrode microstructure [19]. We can see that the combination of neural networks and other methods has distinct advantages in predicting SOFC performance.

With the progress of science and technology, some studies have found that biological dendrites also participate in biological neural network calculations [20]. There are three types of processing units in the network: input unit, output unit, and hidden unit. This traditional neural network structure has higher requirements for selecting hidden units and increases the computational burden for predicting results [21]. In order to effectively address the issues stemming from hidden units, some scholars have found that dendritic networks possess stronger adaptive abilities [22]. To confirm the benefits of this algorithm in neural networks, Gang conducted numerous experiments using datasets to verify its efficacy [23].

In addition to the structure of the neural network, optimization methods also affect the prediction ability of neural networks. Among the existing neural network optimization algorithms, adaptive moment estimation is widely adopted. However, they still have disadvantages for the convergence of optimal solutions. Iiduka used learning rate to improve the optimization efficiency of adaptive mean square gradient and adaptive moment estimation in neural networks [24]. In addition, Iiduka also optimized the approximation algorithm through Adam to realize the constrained nonconvex random finite sum and online optimization in deep neural networks [25]. Xiao used adaptive moment estimation to improve the quality of image generation in the computer vision field [26]. Based on the above outstanding contributions, in order to better predict SOFC system thermoelectric efficiency, this study proposes an improved adaptive neural network method based on dendrite net and AMSG hybrid methods for an SOFC system, which is called the DAG method [23,27]. The advantage of the DAG method is that it can balance the logical relationships between variables in the state of insufficient historical data and obtain reliable data through compensation. In addition, its adaptive characteristics also have great universality for systems with multivariable coupling characteristics, which are the main reasons for adopting this method. When the SOFC system dendrite network is trained, the AMSG method is adopted to tune the weight matrix for increasing DN model prediction accuracy. Then the DAG method is applied to the SOFC system. When the DAG model is used, errors in the thermoelectric efficiency predictive model of the SOFC system can be avoided due to insufficient hidden unit nodes. In addition, the evaluation indices based on mean absolute error (MAE) and root mean squared error (RMSE) prove the effectiveness of DAG method in predicting the thermoelectric efficiency of two SOFC system examples. The main contributions of this study are as follows:

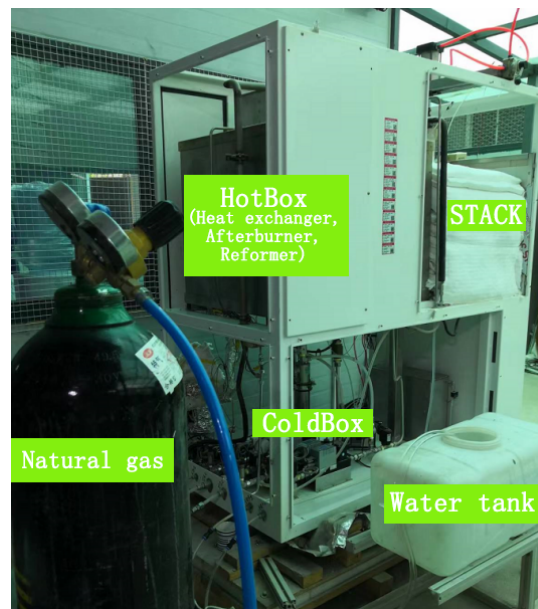
- The number of neural network hidden units used to predict SOFC system efficiency is adaptive.
- This method is used to study the heat efficiency (HE) and electrical efficiency (EE) of an SOFC system. Compared with dendrite net (DN), back propagation (BP), support vector machine (SVM), random forest (RF), genetic algorithm-radial basis function (GA-RBF), artificial neural network (ANN), radial basis function (RBF), genetic algorithm-back propagation (GA-BP), and least squares-support vector machine (LS-SVM), the prediction accuracy of the used method is better. In addition, the system efficiency optimization direction is also determined.
- The SOFC system load tracking process is studied. Compared with BP, genetic algorithm-least squares support vector regression (GA-LSSVR), support vector regression (SVR), DN, long short-term memory (LSTM), stacked long-short term memory (S-LSTM), sparse pseudo-input Gaussian process (SPGP), stack-artificial neural net-

work (stk-ANN), and extreme learning machine (ELM), the DAG method has higher prediction accuracy. Based on the results of the two experiments, it is found that in terms of predicting thermoelectric efficiency, the comprehensive MAE and RMSE values are both lower than 0.014, significantly better than other methods. In addition, through SOFC system samples analysis, optimizing the operating point will help improve system thermoelectric efficiency.

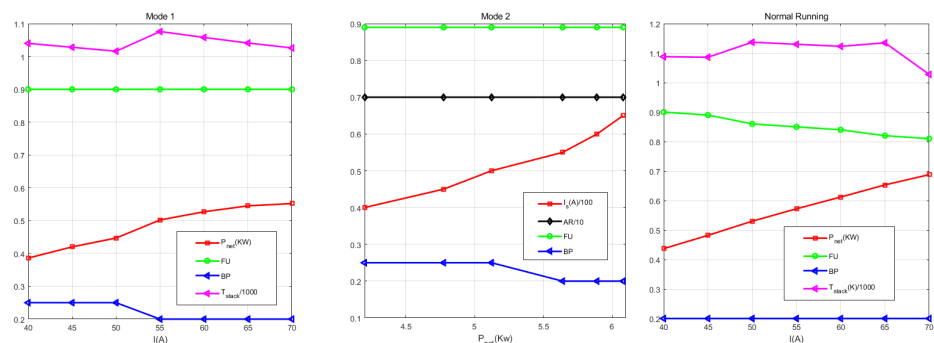
2. Problem Formulation and Methodology

2.1. Problem of SOFC System Efficiency Prediction

SOFC systems have multiple operation points matching one system efficiency point. The system efficiency is time-varying. In order to quickly find the operational point that matches the system efficiency, this study conducts efficiency prediction for the SOFC system, as depicted in Figure 1a [28]. Once the efficiency prediction is completed, the operational points are matched over time to promptly adjust the system efficiency.



(a)



(b)

Figure 1. SOFC system physical object and multi-objective mapping problem ((a) SOFC system physical diagram; (b) Schematic diagram of multi-objective mapping).

From Figure 1b, the fuel utilization (FU) of the SOFC system is obviously different when the SOFC system is under different bypass (BPs) valve opening, temperature, current, and power conditions. Therefore, designing a thermoelectric efficiency prediction method for the SOFC system is crucial for enhancing high-efficiency power generation. To stream-

line the research, the efficiency prediction modeling in this study temporarily disregards the impact introduced by BPs valve opening.

2.2. DAG Method

2.2.1. Traditional DN Method

The framework structure of the DN method is shown in Figure 2. From Figure 2, we can know that there is a great difference between the DN network and traditional neural network structure [27].

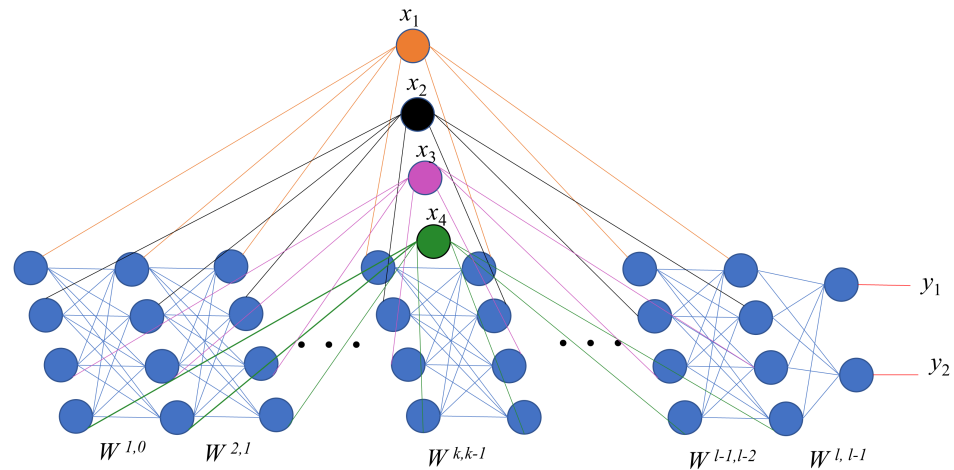


Figure 2. Architecture of the DN method.

The traditional DN method equation is composed of Equations (1)–(8) [29]. The DN output T^k value is shown in Equation (1).

$$T^k = W^{k,k-1} T^{k-1} \circ X \tag{1}$$

where T^{k-1} is the input of DN, \circ represents the Hadamard product; X is the input value after standardization; and W is the weight matrix for tuning neural network stability. System output is shown in Equation (2),

$$Y = W^{l,l-1} \left(\dots W^{k,k-1} \left(W^{2,1} \left(W^{1,0} X \circ X \right) \circ X \dots \right) \circ X \dots \right) \tag{2}$$

where X and Y represent input and output of the SOFC system, respectively; $k < l$; W is the weight matrix; and l is the number of relative units. Matrix W is used for updating the DN network iteration effect based on back propagation learning error (Figure 3).

From Figure 3, the DN method forward propagation can be obtained from Equation (3):

$$\begin{cases} T^k = W^{k,k-1} T^{k-1} \circ X \\ T^l = W^{l,l-1} T^{l-1} \end{cases} \tag{3}$$

where $k < l$. Then, the DN error back propagation can be rewritten in Equations (4)–(6):

$$dT^l = \hat{Y} - Y \tag{4}$$

$$\begin{cases} dZ^l = dT^l \\ dZ^k = dT^k \circ X \end{cases} \tag{5}$$

$$dT^{k-1} = \left(T^{k,k-1} \right)^T dZ^k \tag{6}$$

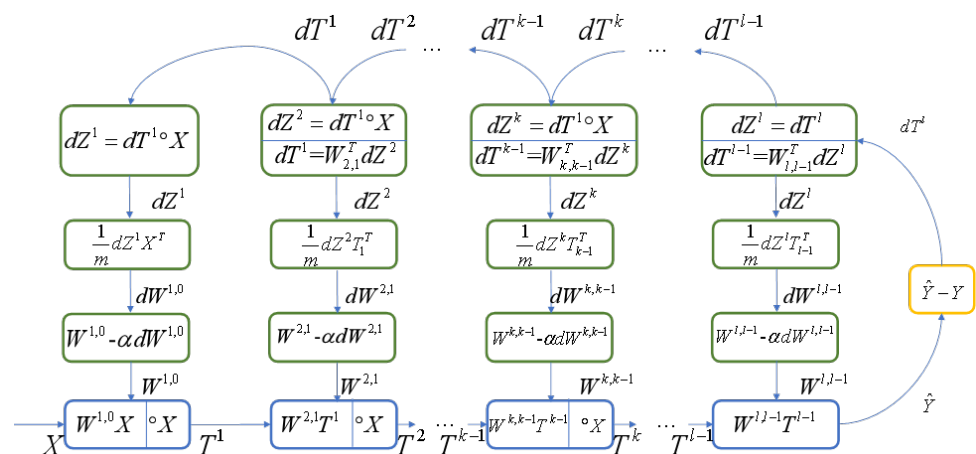


Figure 3. Flow chart of back propagation rules for the error learning rate.

According to Equations (7) and (8), the weight matrix parameter W real-time value can be found.

$$dW^{k,k-1} = dZ^k \left(T^{k,k-1} \right)^T / m \tag{7}$$

$$W^{k,k-1} = W^{k+1,k} - \alpha dW^{k,k-1} \tag{8}$$

where α represents the learning rate of this method, Y represents the data label of the SOFC system, \hat{Y} is the SOFC system predictive DN model output, and m represents the number of set batches in the training process.

2.2.2. AMSG Algorithm

Yu proposed the AMSG method to improve prediction accuracy. This method performs well in completing the optimal solution [30]. Therefore, this study also uses this method to improve the DN model effect for the SOFC system. The AMSG method equation is composed of Equations (9)–(12) [30].

The detailed calculation Equations (9) and (10) are as follows:

$$m_t = \beta_1 m_{t-1} + (1 - \beta_1) g_t \tag{9}$$

$$V_t = \beta_2 V_{t-1} + (1 - \beta_2) g_t^2 \tag{10}$$

where β_1 and β_2 are the degradation rates, and these value are usually set to 0.9 and 0.999, respectively. In addition, t is the iteration times, g_t is the gradient value, m is used to stabilize the gradient, and V is an adaptive gradient parameter. In addition, the tuning parameter can be found using Equations (11) and (12),

$$\hat{V}_t = \max(\hat{V}_t - 1, V_t) \tag{11}$$

$$\theta_{t+1} = \theta_t - ((\alpha m_t) / (\epsilon + \sqrt{\hat{V}_t})) \tag{12}$$

where \max refers to the maximum value, and ϵ is a constant: its value is usually small, so as to maintain numerical stability. Moreover, α is the learning rate, upper mark \wedge is a predictive value, and θ_t and θ_{t+1} are the weight matrix of iteration t and $t + 1$, respectively.

2.2.3. DAG Method Operation Process

In order to obtain the high accuracy SOFC system predictive efficiency, this study uses the AMMSG method in Section 2.2 to obtain the weight matrix [27]. The DAG method detailed steps are as follows [31]:

Step 1: Normalize the original dataset of SOFC system operation through Equation (13) [31].

$$y = y_{\min} + ((y_{\max} - y_{\min}) * (x - x_{\min}) / (x_{\max} - x_{\min})) \tag{13}$$

where x and y are the input data and output data, respectively. Therefore, x_{\max} and x_{\min} are the maximum value and minimum value of input data; y_{\max} and y_{\min} are also the maximum value and the minimum value, respectively.

Step 2: Input the training data into the SOFC system with the DAG method based on Equation (3), and the current neural network unit output is the next network unit input.

Step 3: The SOFC system thermoelectric efficiency model gradient is found from Equations (4)–(7).

Step 4: Update the weight matrix W using Equations (9)–(12). Finally, the DAG model is obtained through multiple iterative training. Then the DAG model predictive effect can be evaluated using RMSE and MAE from Equations (14) and (15) [32].

$$RMSE^2 = n^{-1} * \sum_{i=1}^n (\hat{Y}(i) - Y(i))^2 \tag{14}$$

$$MAE(x, h) = n^{-1} * \sum_{i=1}^n |h(x^i - y^i)| \tag{15}$$

where \hat{Y} and Y represents the predicted output and the expected output of SOFC system efficiency, respectively, and n is the number of data.

Step 5: Input test data into the SOFC system DAG model to get thermoelectric efficiency output value. The key index RMSE and MAE are adopted to assess SOFC system DAG model predictive ability.

Step 6: The DAG model output is used to analyze SOFC system efficiency to achieve efficiency improvement.

The flow chart of DAG is shown in Figure 4:

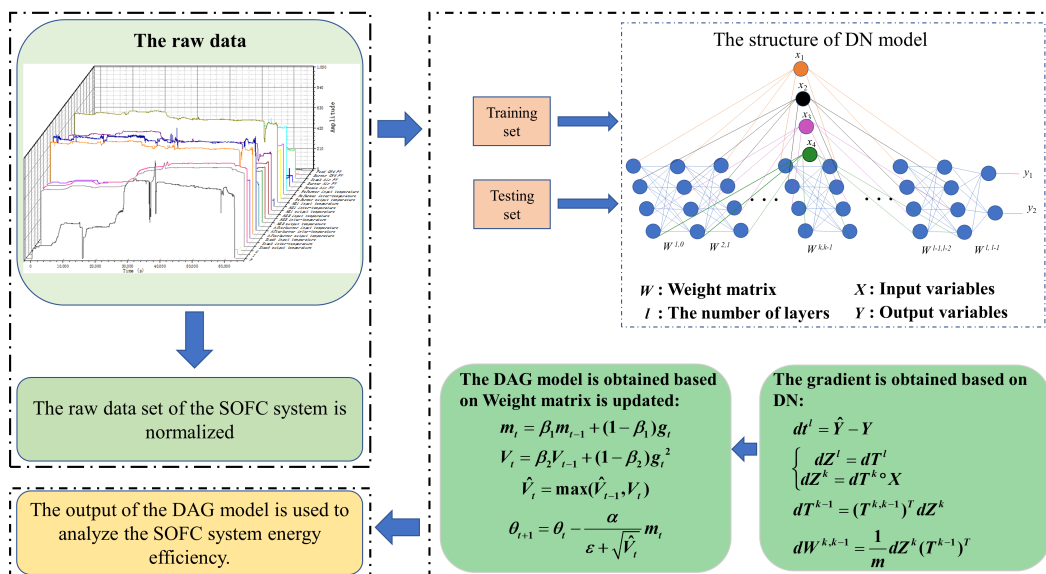


Figure 4. DAG method flow chart.

In addition, in order to further verify the reliability of this method, we need to use a secondary experiment of the SOFC system to verify the method used. Please refer to Section 3.2 for specific verification methods and results.

2.3. Thermoelectric Data Collection of the SOFC System

Discharge and heat supply are the main forms of SOFC system energy conversion [28]. Analyzing the impact of discharge and heating is helpful to find a reasonable operation point, which can effectively reduce SOFC system energy loss and realize system efficiency improvement [33].

Wu used the SOFC system to generate a dataset for predicting and analyzing discharge and heating of the SOFC system [28]. In this dataset, the rated power of SOFC systems is 1 kW, but the experimental time and duration are not equal. The materials, gas supply, component composition, load, and air pressure of the SOFC system are the same. The layout of the SOFC system's BOP components, as well as detailed information about inputs, outputs, and the working environment, are shown in Figure 5.

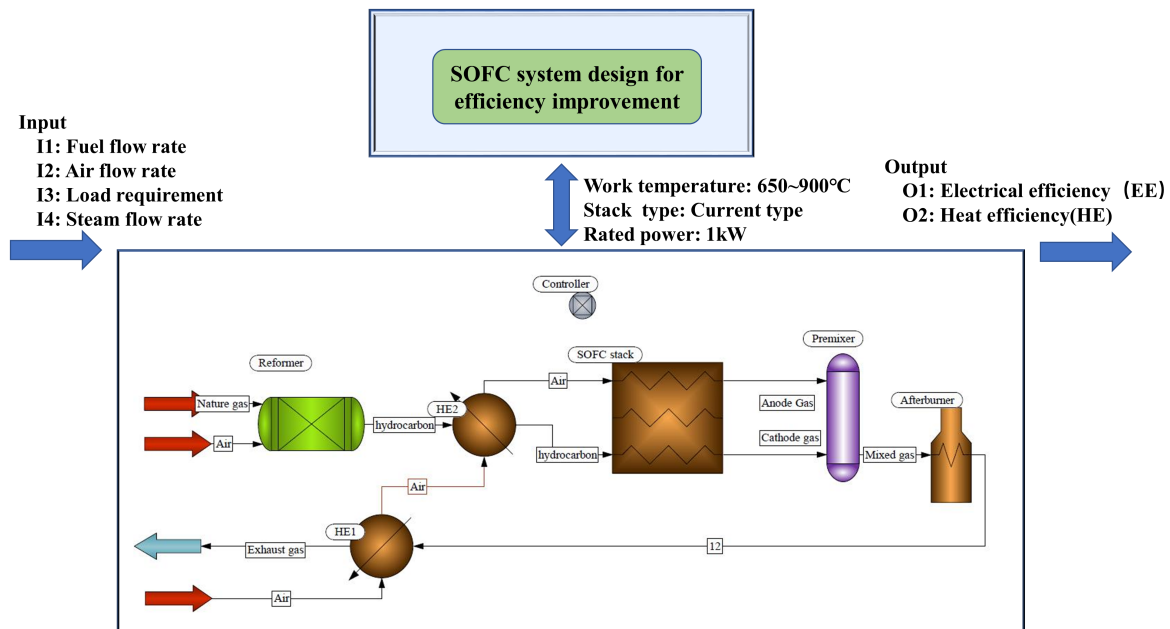


Figure 5. SOFC system simulation detailed information chart.

In addition, in order to obtain the thermoelectric efficiency of the SOFC system, the calculation method adopted in this study is as shown in Equations (16) and (17) [34]:

$$EE = \left(\frac{LHV * \dot{N}_i}{t * \mathfrak{S}} \right)^{-1} * I * V * N_{cell} * 100\% \quad (16)$$

$$HE = V_{water} * C_{water} * \Delta T_{water} \quad (17)$$

where LHV is low heat value of fuel; \dot{N}_i represents fuel flow rate; t represent the time, which has a conversion relationship between it and the flow rate that would depend on the circumstances; I is the current of the SOFC stack; V is the voltage of the SOFC stack; N is the number of cells in the SOFC stack; and \mathfrak{S} is a conversion factor to calculate electrical efficiency for the SOFC system. In addition, V_{water} is the exhaust water volume, C is specific heat capacity, and ΔT is temperature change value. The water is used to deal with high temperature exhaust gas for SOFC system external environment safety.

Each SOFC system condition is represented by four input indices, as shown in Figure 5. There are four features represented by I1 to I4, respectively. At the same time, we record each SOFC system HE and EE. Some data of the SOFC system are shown in Figure 6 (Figure 6 is a high-definition version of the small image in the upper left corner of Figure 4), and the system efficiency is shown in Figure 7. The relevant model setting parameters are shown in the left half of Table 1. The right side shows the stack and time parameters used in the two experiments (Time 1 is the experimental parameter of Figures 6 and 7).

Table 1. Key parameters.

Key Parameters		
Model parameters	Number of inputs	4
	Number of outputs	2
	β_1	0.9
	β_2	0.999
	ε	0.01
	α	0.0001
	\mathfrak{S}	0.278 L·(mol·min ⁻¹)
Experimental parameters	C	4.2 KJ/(kg·°C)
	The number of cells	24
	Effective working area	169 cm ²
	Actual size	225 cm ²
	Duration of operation (Time 1)	682 h
	Duration of operation (Time 2)	1099 h

In Table 1, the effective working area represents the size of the fuel cell as 13 cm × 13 cm, whereas the actual size includes the uncoated area on the edges, which is 15 cm × 15 cm. Therefore, the effective working area is 169 cm², and the actual size is 225 cm².

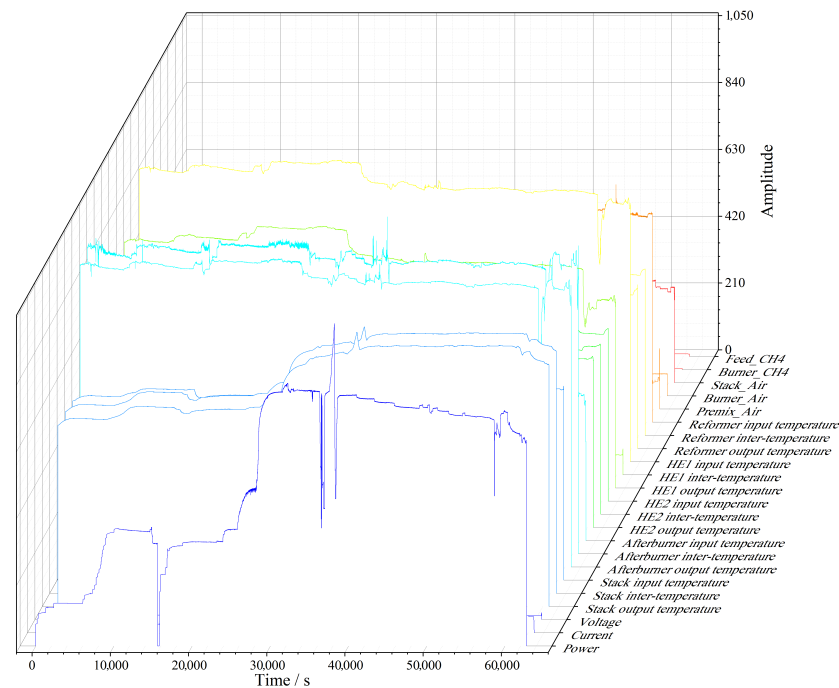


Figure 6. Original sample set of the SOFC system.

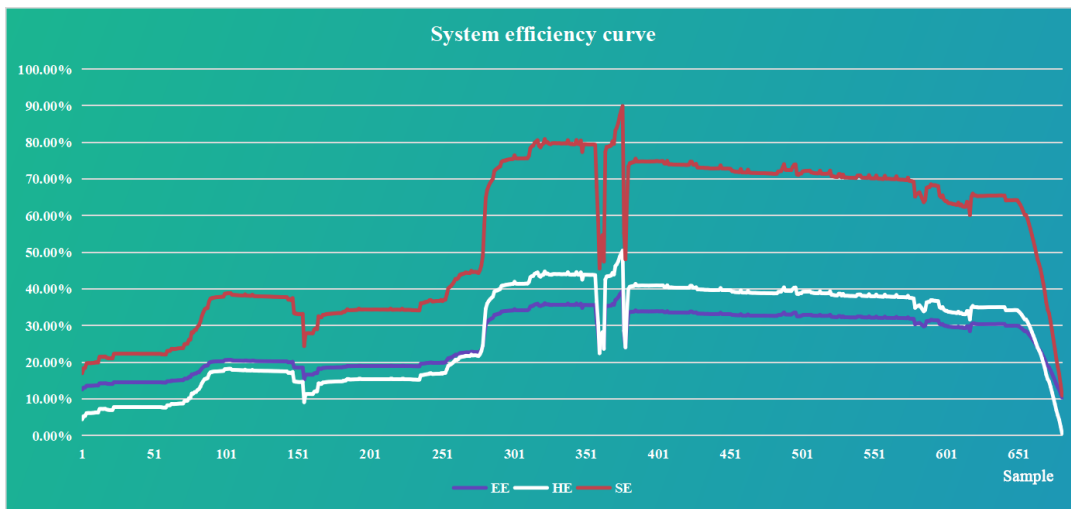


Figure 7. SOFC system efficiency sample set.

3. Results and Discussion

3.1. SOFC System Thermoelectric Efficiency Predictive Modeling Result and Analysis

When the model is built, the training data have 614 h and the test data have 68 h. In order to test the DAG model effectiveness proposed in this study, we also use other common methods to compare predictive effect with ANN [19], BP neural network [35], GA-RBF neural network [36], GA-BP [37], and LS-SVM [38]. Compared with the experimental results of the DAG method in this study, the specific index effect is shown in Figure 8. The evaluation index of HE and EE prediction models are RMSE and MAE.

From Figure 8, the DAG method key assessment index RMSE and MAE are near to GA-BP neural network assessment index. Their MAE and RMSE indices are much lower than 0.10, and the RMSE and MAE of DAG are less than DN, SVM, RF, and GA-RBF. In addition, the RMSE of the DAG method is smaller than ANN, RBF, and LS-SVM. Although GA-RBF, ANN, and LS-SVM are smaller than DAG in the MAE index, the RMSE index is more wrong than the DAG method. Thus, the DAG method is better, and the experimental results can be considered to be competitive.

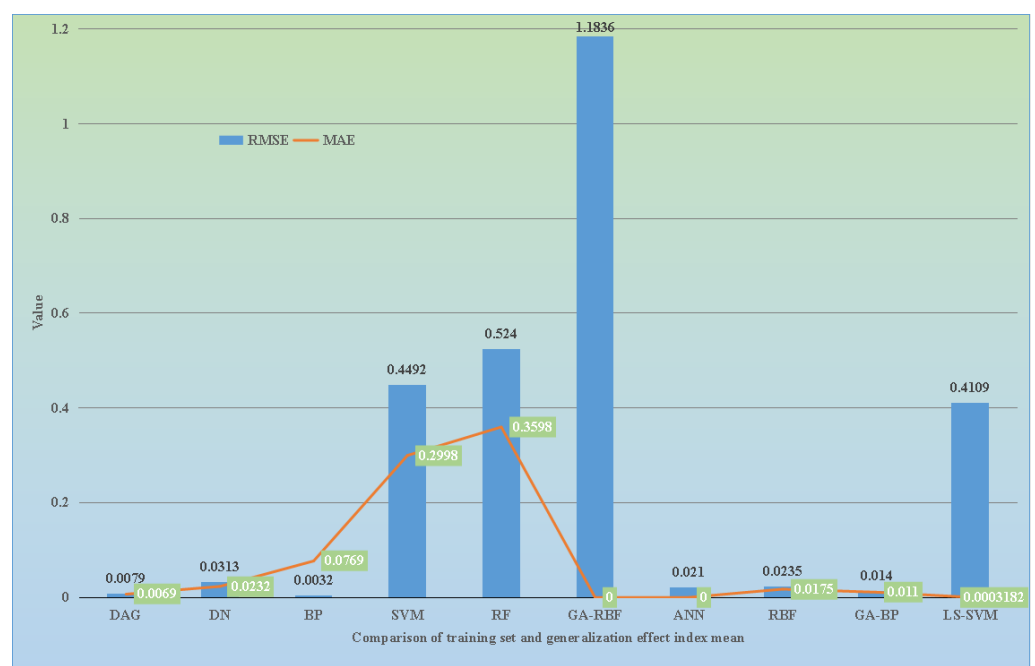


Figure 8. Comparison between the DAG method and other methods using RMSE and MAE.

From Figures 8 and 9, the DAG method prediction accuracy is better than that of other methods on SOFC system's HE and EE, which preliminary proves that the DAG method predictive effect is very significant. Specifically, from Figure 8, both MAE and RMSE values of the DAG method are less than 0.01, which has significant advantages compared to other methods. Other methods either have all values greater than 0.01 or only a single value less than 0.01. From Figure 9, the predicted output tends to be consistent with the expected output, indicating good predictive performance.

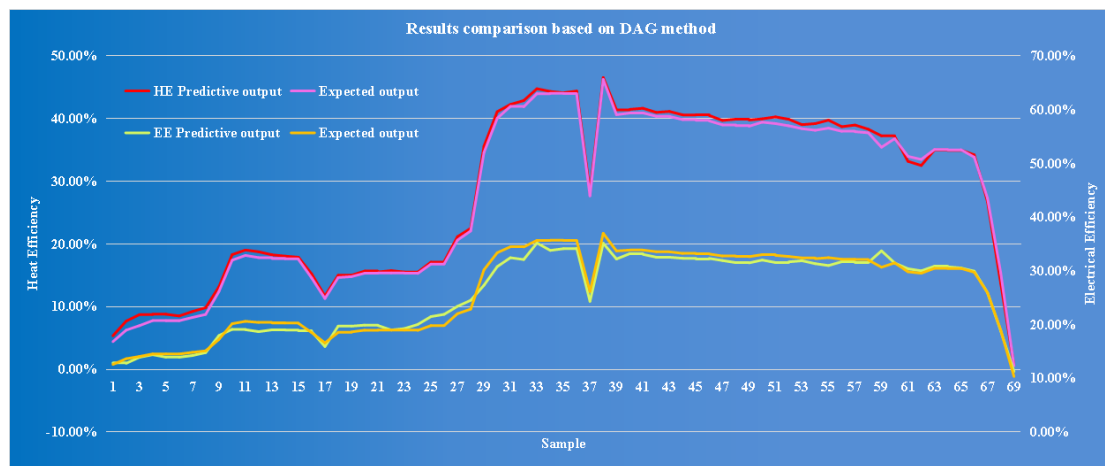


Figure 9. Expected and predicted outputs of HE and EE (using the DAG method).

It should be noted here that the expected output actually represents the measured value from the system experimental platform.

In order to analyze the SOFC system efficiency more effectively, this study mainly analyzes system efficiency after entering the normal power generation stage (the sample point interval is from 30 to 66). In the prediction data, the maximum values of HE and EE at the 38th sample point are 46.56% and 35.15%, respectively. For heat efficiency, the predicted value is greater than the expected value (46.26%). For electrical efficiency, the predicted EE value is less than the expected value (37%), which indicates the direction of SOFC system efficiency optimization in the future. The direction is to further improve SOFC system electrical efficiency. The 37th predicted sample point HE and EE values are 28.29% and 24.32%, respectively. Their value is also higher than the expected HE value (27.68%) and lower than the expected EE value (26.16%). The results show that when the SOFC system has abnormal working conditions, the EE has potential to increase. Therefore, when designing an SOFC system, the structural scheme can be adjusted according to the above results, so as to reduce SOFC system energy loss and increase electrical efficiency. For example, an afterburner with low power can be selected to reduce SOFC system heat efficiency.

3.2. Second Verification of Proposed Method Effectiveness for the SOFC System

The equipment is located in the fuel cell research center of Huazhong University of science and technology, and the system is a 1 kW SOFC system [39]. The system architecture is shown in Figure 10, which is divided into a hotbox and a coldbox. Each BOP component is equipped with temperature, pressure, and flow rate sensors to collect key parameter information. The BOP component installation orientation of the SOFC system coldbox and hotbox are shown in Figure 10. In addition, the electrical signal sensor is installed on both sides of the load. In Figure 10, the sensors are represented by a circle and English letters: T is temperature sensor, P is pressure sensor, and R is gas flow rate sensor. These data are mainly from industrial computer stations. Time 2 is the second experimental parameter in Table 1.

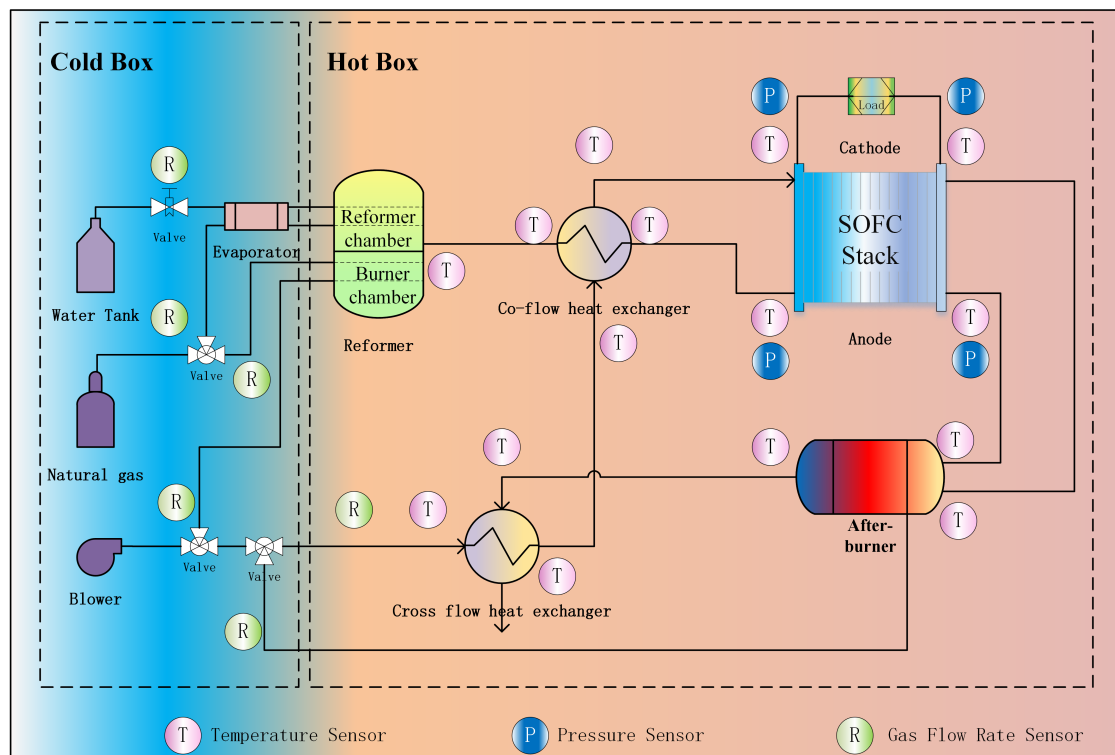


Figure 10. SOFC system distribution and sensor installation position.

3.3. Thermoelectric Efficiency Analysis of the SOFC System

3.3.1. Efficiency Analysis

In Figure 10, when the SOFC system performs a load tracking task, its thermoelectric efficiency is taken as the output, and the input is the same as that in Figure 5. These input and output variables are used to train and test the DAG model. A total of 1099 datasets are used this time. Among them, there are 1000 training sets and 99 test sets [37]. Then, a new set of data are used to verify the DAG method availability by using eight methods. This time, the data are still from the fuel cell research center of Huazhong University of science and technology. The DAG method is compared with other methods such as ELM [40], GA-LSSVR [41], SVR [42], S-LSTM [43], SPGP [44], and stk-ANN [45]. The comparison index parameters are MAE and RMSE. The different results comparison are shown in Figure 11.

From Figure 11, stk-ANN and GA-LSSVR are reduced to 0.2 times in order to easily observe the difference between these methods. The RMSE values of stk-ANN and GA-LSSVR are much larger than those of the DAG method, which indicates that these methods have overfitting. The MAE values of LSTM, S-LSTM, and stk-ANN are much larger than those of the DAG method. Through comparison, MAE and RMSE values are more reasonable, and the DAG method is proved again to have the highest prediction accuracy for the SOFC system.

In the prediction data, the EE value of the 970th sample point is 46.92%, higher than the expected value of 46.17%. The predicted EE value of the 220th sample point is 42.13%, and its expected value is 42.12%. The two data are very close. Two samples show the direction optimization of SOFC system efficiency.

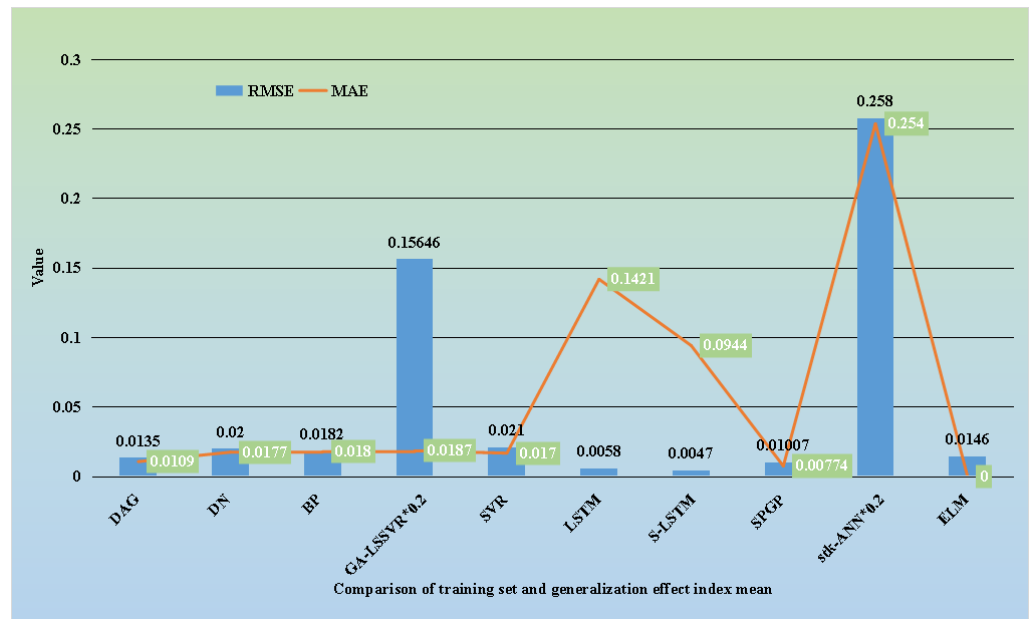


Figure 11. Analysis results comparison of second dataset using the DAG method.

3.3.2. System Efficiency Improvement and Carbon Emission Reduction Measures

When SOFC system efficiency needs to be adjusted, we can first compare the difference between the actual efficiency and the expected efficiency based on the adjustment process in Figure 12, and then we can adjust operating points I1~I4 of the expected efficiency. The adjustment sequence is adjusted according to the process of I3 (load)~I1 (fuel flow rate)~I4 (steam flow rate)~I2 (air flow rate). In the process of regulation, if SOFC system real efficiency is close or matches the expected efficiency, the regulation can be terminated at any time to maintain the system working state.

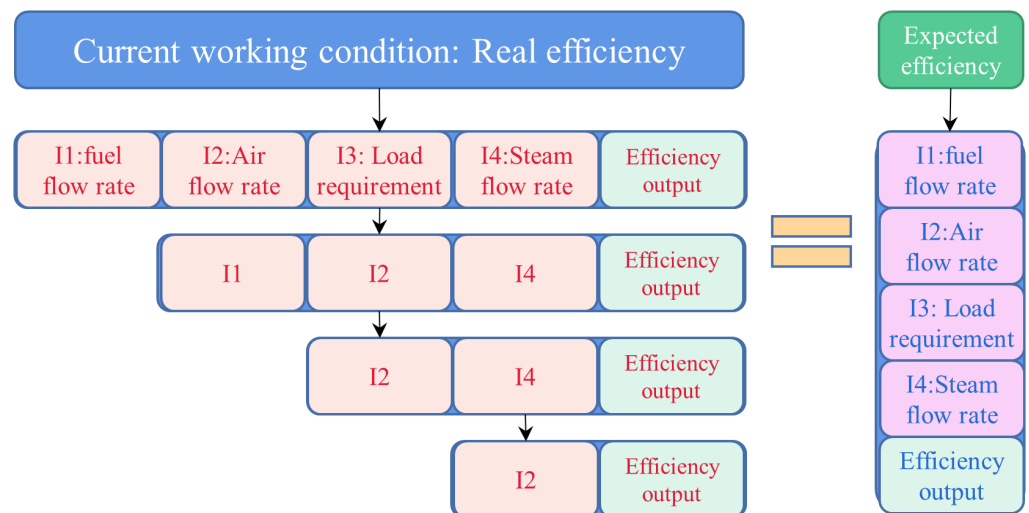


Figure 12. System efficiency optimization process.

In the process of SOFC system thermoelectric efficiency switching, the large difference in switching time scales between electric efficiency and thermal efficiency cannot be avoided. Thus, we need to fully study the control strategy, which will be our future research object. In addition, we can install carbon capture devices at the system exhaust gas outlet to reduce carbon emissions.

4. Conclusions

In this study, a new adaptive neural network is proposed to predict SOFC system energy loss. The prediction results of the model are used to guide the operation point adjustment of system efficiency optimization. In the novel adaptive neural network, its hidden unit does not need to be determined in advance and can be trained automatically. With neural network weight adjustment, the AMMSG is used to optimize the DN model, then a good DAG model is obtained, which further proves the superiority of this method. Comparison with methods in other literature, this proposed method has better predictive ability for SOFC system thermoelectric efficiency. After prediction and analysis, we find the proposed method has the lowest MAE and RMSE values (less than 0.014). The result is the guiding direction for SOFC system efficiency optimization. After the SOFC system operation point is optimized, installing a carbon capture device at the end of the SOFC system can achieve the dual effects on emission reduction and efficiency. The research outcome of this study can provide guidance for fuel cell vehicles and boats efficiency optimization and contribute to sustainable development of the environment.

In the future, we will refer to more mature neural network methods to conduct a more in-depth study on the operation efficiency optimization of the SOFC system, further improve the efficiency prediction model used, and design relevant control strategies to achieve a more effective improvement for SOFC system thermoelectric efficiency.

Author Contributions: Conceptualization and methodology, X.W. and X.L.; validation, X.W.; formal analysis, Y.W.; writing—original draft preparation, Y.W.; writing—review and editing, Y.W., Y.X. and Y.C.; supervision, X.W. and X.L.; project administration, X.L.; funding acquisition, X.W. and X.L. All authors have read and agreed to the published version of the manuscript.

Funding: This research was funded by the National Natural Science Foundation of China (grant no. 62203204, U2066202), Jiangxi Provincial Natural Science Foundation (grant no. 20232BAB202028, 20212BAB212013), China Postdoctoral Science Foundation Funded Project (Grant no. 2023M732387), and Belt and Road Joint Laboratory on Measurement and Control Technology Fund (No. mct202102).

Institutional Review Board Statement: Not applicable.

Informed Consent Statement: Not applicable.

Data Availability Statement: Data are available on reasonable demand from the corresponding author.

Acknowledgments: We are very grateful to Jakub Kupecki from Center for Hydrogen Technologies (CTH2), Institute of Power Engineering in Poland for their technical support to this article.

Conflicts of Interest: The authors declare no conflict of interest.

Nomenclature

Explanation of abbreviation in manuscript

<i>AMSG</i>	Adaptive mean square gradient
<i>LS-SVR</i>	Least squares support vector regression
<i>ANN</i>	Artificial neural networks
<i>LSTM</i>	Long short-term memory
<i>BP</i>	Back propagation
<i>MAE</i>	Mean absolute error
<i>DN</i>	Dendrite net
<i>RBF</i>	Radial basis function
<i>DAG</i>	Dendrite net based on the AMMSG
<i>RF</i>	Random forest
<i>EE</i>	Electrical efficiency
<i>RMSE</i>	Root mean square error
<i>ELM</i>	Extreme learning machine
<i>SPGP</i>	Sparse pseudo-input Gaussian process

GA	Genetic algorithm
stk-ANN	Stack-artificial neural network
HE	Heat efficiency
SVM	Support vector machine
LS	Least squares
SVR	Support vector regression
X	Input value after standardization
Y	Output value after standardization
x	Input value before standardization
y	Output value before standardization
T	DN input or output
W	Weight matrix or tuning neural network stability
k	The number of relative units
l	The number of relative units
Z	Transition matrix
α	Learning rate
\hat{Y}	Model output predictive value
m	The number of set batches in the training process
β	Degradation rate
t	Iteration times or operate time
θ	Iteration weight matrix
g_t	Adaptive gradient value
$\hat{\cdot}$	Predictive value
V	Adaptive gradient parameter or stack voltage
ε	Setting parameter
LHV	Low heat value
\dot{N}	Gas flow rate
I	Current
N	The number of cells
V_{water}	Volume of water
C	Specific heat capacity
ξ	Conversion factor
Δ	Change rate
\circ	Hadamard product

References

- Shang, Z.; Hossain, M.M.; Wycisk, R.; Pintauro, P.N. Poly (phenylene sulfonic acid)-expanded polytetrafluoroethylene composite membrane for low relative humidity operation in hydrogen fuel cells. *J. Power Sources* **2022**, *535*, 231375. [[CrossRef](#)]
- Zhang, Y.; Chen, B.; Guan, D.; Xu, M.; Ran, R.; Ni, M.; Zhou, W.; O'Hayre, R.; Shao, Z. Thermal-expansion offset for high-performance fuel cell cathodes. *Nature* **2021**, *591*, 246–251. [[CrossRef](#)] [[PubMed](#)]
- Wu, X.L.; Xu, Y.W.; Li, D.; Zheng, Y.; Li, J.; Sorrentino, M.; Yu, Y.; Wan, X.; Hu, L.; Zou, C.; et al. Afterburner temperature safety assessment for solid oxide fuel cell system based on computational fluid dynamics. *J. Power Sources* **2021**, *496*, 229837. [[CrossRef](#)]
- Rezk, H.; Olabi, A.; Abdelkareem, M.A.; Maghrabie, H.M.; Sayed, E.T. Fuzzy Modelling and Optimization of Yeast-MFC for Simultaneous Wastewater Treatment and Electrical Energy Production. *Sustainability* **2023**, *15*, 1878. [[CrossRef](#)]
- Corigliano, O.; Pagnotta, L.; Fragiaco, P. On the technology of solid oxide fuel cell (SOFC) energy systems for stationary power generation: A review. *Sustainability* **2022**, *14*, 15276. [[CrossRef](#)]
- Wang, Q.; Wei, H.H.; Xu, Q. A solid oxide fuel cell (SOFC)-based biogas-from-waste generation system for residential buildings in China: A feasibility study. *Sustainability* **2018**, *10*, 2395. [[CrossRef](#)]
- Slater, J.; Chronopoulos, T.; Panesar, R.; Fitzgerald, F.; Garcia, M. Review and techno-economic assessment of fuel cell technologies with CO₂ capture. *Int. J. Greenh. Gas Control* **2019**, *91*, 102818. [[CrossRef](#)]
- Wang, F.; Deng, S.; Zhang, H.; Wang, J.; Zhao, J.; Miao, H.; Yuan, J.; Yan, J. A comprehensive review on high-temperature fuel cells with carbon capture. *Appl. Energy* **2020**, *275*, 115342. [[CrossRef](#)]
- Huo, H.; Xu, K.; Cui, L.; Zhang, H.; Xu, J.; Kuang, X. Temperature gradient control of the solid oxide fuel cell under variable load. *ACS Omega* **2021**, *6*, 27610–27619. [[CrossRef](#)]
- Wu, Z.; Tan, P.; Chen, B.; Cai, W.; Chen, M.; Xu, X.; Zhang, Z.; Ni, M. Dynamic modeling and operation strategy of an NG-fueled SOFC-WGS-TSA-PEMFC hybrid energy conversion system for fuel cell vehicle by using MATLAB/SIMULINK. *Energy* **2019**, *175*, 567–579. [[CrossRef](#)]

11. Huo, W.; Li, W.; Zhang, Z.; Sun, C.; Zhou, F.; Gong, G. Performance prediction of proton-exchange membrane fuel cell based on convolutional neural network and random forest feature selection. *Energy Convers. Manag.* **2021**, *243*, 114367. [[CrossRef](#)]
12. Wilberforce, T.; Olabi, A. Proton exchange membrane fuel cell performance prediction using artificial neural network. *Int. J. Hydrogen Energy* **2021**, *46*, 6037–6050. [[CrossRef](#)]
13. Chen, K.; Laghrouche, S.; Djerdir, A. Degradation prediction of proton exchange membrane fuel cell based on grey neural network model and particle swarm optimization. *Energy Convers. Manag.* **2019**, *195*, 810–818. [[CrossRef](#)]
14. Xie, R.; Ma, R.; Pu, S.; Xu, L.; Zhao, D.; Huangfu, Y. Prognostic for fuel cell based on particle filter and recurrent neural network fusion structure. *Energy AI* **2020**, *2*, 100017. [[CrossRef](#)]
15. Buchaniec, S.; Gnatowski, M.; Hasegawa, H.; Brus, G. A Surrogate Model of the Butler-Volmer Equation for the Prediction of Thermodynamic Losses of Solid Oxide Fuel Cell Electrode. *Energies* **2023**, *16*, 5651. [[CrossRef](#)]
16. Subotić, V.; Eibl, M.; Hochenauer, C. Artificial intelligence for time-efficient prediction and optimization of solid oxide fuel cell performances. *Energy Convers. Manag.* **2021**, *230*, 113764. [[CrossRef](#)]
17. Ba, S.; Xia, D.; Gibbons, E.M. Model identification and strategy application for Solid Oxide Fuel Cell using Rotor Hopfield Neural Network based on a novel optimization method. *Int. J. Hydrogen Energy* **2020**, *45*, 27694–27704. [[CrossRef](#)]
18. Gnatowski, M.; Buchaniec, S.; Brus, G. The prediction of the polarization curves of a solid oxide fuel cell anode with an artificial neural network supported numerical simulation. *Int. J. Hydrogen Energy* **2023**, *48*, 11823–11830. [[CrossRef](#)]
19. Yan, Z.; He, A.; Hara, S.; Shikazono, N. Modeling of solid oxide fuel cell (SOFC) electrodes from fabrication to operation: Microstructure optimization via artificial neural networks and multi-objective genetic algorithms. *Energy Convers. Manag.* **2019**, *198*, 111916. [[CrossRef](#)]
20. Brus, G. Overcoming a recent impasse in the application of artificial neural networks as solid oxide fuel cells simulator with computational topology. *Energy AI* **2023**, *14*, 100291. [[CrossRef](#)]
21. Xu, H.; Ma, J.; Tan, P.; Chen, B.; Wu, Z.; Zhang, Y.; Wang, H.; Xuan, J.; Ni, M. Towards online optimisation of solid oxide fuel cell performance: Combining deep learning with multi-physics simulation. *Energy AI* **2020**, *1*, 100003. [[CrossRef](#)]
22. Nguyen, D.D.; Pham, T.Q.D.; Tanveer, M.; Khan, H.; Park, J.W.; Park, C.W.; Kim, G.M. Deep learning-based optimization of a microfluidic membraneless fuel cell for maximum power density via data-driven three-dimensional multiphysics simulation. *Bioresour. Technol.* **2022**, *348*, 126794. [[CrossRef](#)] [[PubMed](#)]
23. Liu, G. It may be time to perfect the neuron of artificial neural network. *Preprints* **2020**, 2020060175.
24. Iiduka, H. Appropriate learning rates of adaptive learning rate optimization algorithms for training deep neural networks. *IEEE Trans. Cybern.* **2021**, *52*, 13250–13261. [[CrossRef](#)] [[PubMed](#)]
25. Iiduka, H. ϵ -Approximation of Adaptive Learning Rate Optimization Algorithms for Constrained Nonconvex Stochastic Optimization. *IEEE Trans. Neural Netw. Learn. Syst.* **2022**, early access.
26. Xiao, Y.; Pun, C.M.; Liu, B. Crafting adversarial example with adaptive root mean square gradient on deep neural networks. *Neurocomputing* **2020**, *389*, 179–195. [[CrossRef](#)]
27. Liu, G.; Wang, J. Dendrite net: A white-box module for classification, regression, and system identification. *IEEE Trans. Cybern.* **2021**, *52*, 13774–13787. [[CrossRef](#)]
28. Wu, X.L.; Xu, Y.W.; Xue, T.; Zhao, D.Q.; Jiang, J.; Deng, Z.; Fu, X.; Li, X. Health state prediction and analysis of SOFC system based on the data-driven entire stage experiment. *Appl. Energy* **2019**, *248*, 126–140. [[CrossRef](#)]
29. Jiang, Y.; Liu, Y.; Yang, Z. Parameter identification of DC–DC converter based on dendrite net under fluctuating input voltages. *IET Power Electron.* **2023**, *16*, 2076–2090. [[CrossRef](#)]
30. Yu, Y.; Liu, F. Effective neural network training with a new weighting mechanism-based optimization algorithm. *IEEE Access* **2019**, *7*, 72403–72410. [[CrossRef](#)]
31. Han, Y.; Li, J.; Lou, X.; Fan, C.; Geng, Z. Energy saving of buildings for reducing carbon dioxide emissions using novel dendrite net integrated adaptive mean square gradient. *Appl. Energy* **2022**, *309*, 118409. [[CrossRef](#)]
32. Chai, T.; Draxler, R.R. Root mean square error (RMSE) or mean absolute error (MAE). *Geosci. Model Dev. Discuss.* **2014**, *7*, 1525–1534.
33. Zhang, L.; Li, X.; Jiang, J.; Li, S.; Yang, J.; Li, J. Dynamic modeling and analysis of a 5-kW solid oxide fuel cell system from the perspectives of cooperative control of thermal safety and high efficiency. *Int. J. Hydrogen Energy* **2015**, *40*, 456–476. [[CrossRef](#)]
34. Wu, X.L.; Xu, Y.W.; Zhao, D.Q.; Zhong, X.B.; Li, D.; Jiang, J.; Deng, Z.; Fu, X.; Li, X. Extended-range electric vehicle-oriented thermoelectric surge control of a solid oxide fuel cell system. *Appl. Energy* **2020**, *263*, 114628. [[CrossRef](#)]
35. Song, S.; Xiong, X.; Wu, X.; Xue, Z. Modeling the SOFC by BP neural network algorithm. *Int. J. Hydrogen Energy* **2021**, *46*, 20065–20077. [[CrossRef](#)]
36. Wu, X.J.; Zhu, X.J.; Cao, G.Y.; Tu, H.Y. Predictive control of SOFC based on a GA-RBF neural network model. *J. Power Sources* **2008**, *179*, 232–239. [[CrossRef](#)]
37. Wang, Y.; Qing, D. Model predictive control of nonlinear system based on GA-RBP neural network and improved gradient descent method. *Complexity* **2021**, *2021*, 6622149. [[CrossRef](#)]
38. Zhao, W.; Jiang, J.; Qin, H.; Li, X.; Li, J. Machine learning based soft sensor and long-term calibration scheme: A solid oxide fuel cell system case. *Int. J. Hydrogen Energy* **2021**, *46*, 17322–17342. [[CrossRef](#)]
39. Zheng, Y.; Wu, X.L.; Zhao, D.; Xu, Y.W.; Wang, B.; Zu, Y.; Li, D.; Jiang, J.; Jiang, C.; Fu, X.; et al. Data-driven fault diagnosis method for the safe and stable operation of solid oxide fuel cells system. *J. Power Sources* **2021**, *490*, 229561. [[CrossRef](#)]

40. Yang, B.; Guo, Z.; Yang, Y.; Chen, Y.; Zhang, R.; Su, K.; Shu, H.; Yu, T.; Zhang, X. Extreme learning machine based meta-heuristic algorithms for parameter extraction of solid oxide fuel cells. *Appl. Energy* **2021**, *303*, 117630. [[CrossRef](#)]
41. Huo, H.B.; Ji, Y.; Zhu, X.J.; Kuang, X.H.; Liu, Y.Q. Control-oriented dynamic identification modeling of a planar SOFC stack based on genetic algorithm-least squares support vector regression. *J. Zhejiang Univ. Sci. A* **2014**, *15*, 829–839. [[CrossRef](#)]
42. Legala, A.; Zhao, J.; Li, X. Machine Learning Modeling for Proton Exchange Membrane Fuel Cell Performance. *Energy AI* **2022**, *10*, 100183. [[CrossRef](#)]
43. Wang, F.K.; Cheng, X.B.; Hsiao, K.C. Stacked long short-term memory model for proton exchange membrane fuel cell systems degradation. *J. Power Sources* **2020**, *448*, 227591. [[CrossRef](#)]
44. Deng, H.; Hu, W.; Cao, D.; Chen, W.; Huang, Q.; Chen, Z.; Blaabjerg, F. Degradation trajectories prognosis for PEM fuel cell systems based on Gaussian process regression. *Energy* **2022**, *244*, 122569. [[CrossRef](#)]
45. Fisher, O.; Watson, N.J.; Porcu, L.; Bacon, D.; Rigley, M.; Gomes, R.L. Data-driven modelling of bioprocesses: Data volume, variability, and visualisation for an industrial bioprocess. *Biochem. Eng. J.* **2022**, *185*, 108499. [[CrossRef](#)]

Disclaimer/Publisher’s Note: The statements, opinions and data contained in all publications are solely those of the individual author(s) and contributor(s) and not of MDPI and/or the editor(s). MDPI and/or the editor(s) disclaim responsibility for any injury to people or property resulting from any ideas, methods, instructions or products referred to in the content.